Intrinsically Strain-Broadened Line Shapes for Magnetic-Resonance Absorption within a Non-Kramers Doublet

C. M. Bowden and H. C. Meyer
Solid State Physics Branch, Physical Sciences Laboratory, Redstone Arsena, Alabama 35809
and
P. L. Donoho
Rice University, Houston, Texas 77001
(Received 11 May 1970)

A theoretical model was developed for the line shape of magnetic-resonance absorption for transitions within a non-Kramers doublet (the term *doublet* is used here to denote the $|\Delta M_s| = 2$ transition within a ground triplet) for the point-group symmetries C_{3v} and O_h. This was done for both the acoustical-paramagnetic-resonance and the electron-paramagnetic-resonance line shapes. The asymmetric broadening of the absorption distribution is interpreted on the basis of the spin-lattice coupling. For the case of C_{3v} symmetry, the calculation was done for both electric-rf-field-induced and magnetic-rf-field-induced transitions, the necessary condition for the former being a lack of inversion symmetry.

I. INTRODUCTION

Phonon-induced transitions between the states of a non-Kramers doublet are allowed,[1] and thus, from this standpoint, the non-Kramers ion impurities in diamagnetic host lattices are particularly adapted to study by acoustical-paramagnetic-resonance (APR) techniques. On the other hand, magnetic dipole transitions between the states of a non-Kramers doublet are forbidden; however, electron paramagnetic resonance (EPR) has been observed in many cases.[2,3] In these cases, the absorption is observed with the rf field $\vec{H}_{rf}$ parallel to the axis of symmetry. This is because the states of the doublet are mixed by local perturbations on the basic axial crystalline field symmetry at the paramagnetic-ion sites, thus giving a nonzero transition probability in which the states are coupled via the z component of the spin operator. In some cases, electrically induced transitions dominate the magnetically induced ones.[4,5] This can arise when the non-Kramers ion occupies a site lacking full inversion symmetry.

Due to the existence of a nonzero orbital moment associated with a free non-Kramers ion, a strong spin-lattice interaction is expected in cases where the spin-orbit interaction is large. The local crystal field for such ions inserted as impurities in host lattices is often axial (even for cubic lattices). This may be due to local charge compensation, but also may stem from a Jahn-Teller distortion of the local complex. Thus, in an axial crystal field each J level is split into singlets and doublets. Often the singlet is quite far removed from the doublet.[3,6] The remaining degeneracies may be removed by local strain distortion to lower symmetry than axial. This is observed as a zero-field splitting of the resonance absorption.

In the case of each of the observations in Refs. 2 and 3, the resonance absorption was asymmetrically broadened, indicating an inhomogeneous distribution in the perturbation from axial symmetry. This implies that the perturbations are caused by local strains corresponding to imperfections in the bulk host crystal.[1] Where the broadening is large ($>10^{-4}$ cm^{-1}), a strong spin-lattice interaction is indicated. Thus, a strong spin-phonon coupling is anticipated, giving rise to an observable APR absorption. This is indeed found to be the case[3,6] for $CaF_2:U^{4+}$ and $Al_2O_3:Fe^{2+}$. In such cases, the APR signal is more readily observed than the EPR, since, as pointed out, the transition within a non-Kramers doublet is allowed for phonon-induced transitions, but forbidden for the case in which the probe used is the magnetic field component of a microwave radiation field.

It is expected that non-Kramers impurity ions having a strong spin-lattice interaction would give correspondingly strong APR and observable EPR signals. Such is indeed the case[3] for $CaF_2:U^{4+}$ and[7-9] $MgO:Fe^{2+}$. In these cases, the line shapes may be compared. The shapes are expected to be fundamentally different, since the transition probabilities are determined by entirely different mechanisms. Specifically, the APR transition probability is the same for each spin packet of the absorption distribution, whereas the EPR transition probability depends explicitly upon the local perturbed environment of each ion. A study based on a comparison between the EPR and APR line shapes could lead to a deeper understanding of the mechanisms which cause coupling between the states.

In this paper, we propose a theoretical model for the line shapes of magnetic-resonance absorption

for transitions within a non-Kramers doublet for the point-group symmetries C_{3v} and O_h.[10] The asymmetric broadening of the absorption distribution is interpreted on the basis of the spin-lattice coupling. For the case of C_{3v} symmetry, the calculation was done for both electric-rf-field-induced and magnetic-rf-field-induced transitions, where the symmetry is C_{3v} without and with inversion symmetry, respectively. It is shown that the shapes of the APR and EPR absorptions are fundamentally different, whereas those of the APR and PER (paraelectric resonance) lines are very nearly the same.

II. THEORY

In this calculation, we assume random distributions of the local strains. This will be a good approximation provided the sources of the strains are heterogeneous and can be considered remote. The probability at a given ion site that the perturbation to the local crystal field symmetry is produced by a given set of local strains whose components are $\{e_i\}(i=1,\ldots,6)$ is

$$\prod_{i=1}^{6} p_i(e_i) \quad , \tag{1}$$

where $p_i(e_i)$ is the probability distribution for the strain component e_i. We let the distribution for the absorption for a single ion, the width of which is determined by the lifetime broadening, be $G(\delta E)$ where δE is the energy variation over the density of final states. Then, each ensemble of spins whose local perturbed environment is associated with a given set of strain components $\{e_i\}_i$ makes a contribution to the resonance absorption at $E=h\nu$:

$$\delta I(E) \sim |\langle i|\mathcal{H}_{rf}|f\rangle|^2 G(E-E') \prod_{i=1}^{6} p_i(e_i) \quad , \tag{2}$$

where the first factor on the right is the square of the matrix element of the Hamiltonian for the rf field which connects the initial and final states, and $E'=E'(e_1,\ldots,e_6)$ is the correction to the transition energy resulting from the perturbation produced by the set of strains whose components are $\{e_i\}$. Neglecting extraneous constant factors, the resonance-absorption line shape is then calculated from the integral [1]

$$I(E)=\int_{-\infty}^{\infty} |\langle i|\mathcal{H}_{rf}|f\rangle|^2 G(E-E') \Pi_i p_i(e_i)\, de_i \quad . \tag{3}$$

This constitutes a volume integral over the full six-dimensional configuration space defined by the strain components. However, the Gaussian probability distributions will guarantee only very small contributions from very large strains in the integrand in Eq. (3). Thus, we use the infinite limits in (3) to greatly facilitate the mathematical calculations which are to follow.

The approach presented to this point is basically similar to that done by McMahon.[11] Other methods have been introduced for the calculation of intrinsically strain-broadened line shapes. The most elegant of these was presented by Stoneham[12] for strain broadening caused by first-order effects in which he explicitly incorporates the nature of the sources of strain into the model. This elegant method in its basic assumption does not, however, carry over to the cases where the lowest-order contribution in the strains is second order as in the case for transitions within a non-Kramers doublet.[1]

A. Site Symmetry D_{3d} and C_{3v}: Magnetic Quadrupole and Phonon-Induced Transitions

In the absence of hyperfine interaction, the magnetic-resonance experiments can be interpreted on the basis of an effective spin-1 formalism[1,13,14] in which the effective spin Hamiltonian is

$$\mathcal{H}=g_{\parallel}\beta H_z S_z + g_{\perp}\beta(H_x S_x + H_y S_y) + D[S_z^2 - \tfrac{1}{3}S(S+1)] + \vec{S}\cdot\overleftrightarrow{\tau}\cdot\vec{S} \, , \tag{4}$$

where the axis of quantization is along the symmetry axis. The last term is a perturbation on the local axial crystal field. This term is written explicitly in terms of the elements τ_{ij} of the coupling tensor $\overleftrightarrow{\tau}$,

$$\begin{aligned}\vec{S}\cdot\overleftrightarrow{\tau}\cdot\vec{S} = {} & \tfrac{1}{4}(\tau_{11}+\tau_{22})(S_-S_+ + S_+S_-) + \tau_{33}S_3^2 \\ & + \tfrac{1}{4}[(\tau_{11}-\tau_{22}) - 2i\tau_{12}]S_+^2 \\ & + \tfrac{1}{4}[(\tau_{11}-\tau_{22}) + 2i\tau_{12}]S_-^2 \\ & + \tfrac{1}{2}(\tau_{13}-i\tau_{23})(S_+S_3 + S_3S_+) \\ & + \tfrac{1}{2}(\tau_{13}+i\tau_{23})(S_-S_3 + S_3S_-) \, .\end{aligned} \tag{5}$$

The assumption that these perturbations are caused by local strains e_{kl} is expressed in terms of the elements of the coupling tensor $\overleftrightarrow{\tau}$ by

$$\tau_{ij}=\sum_{kl} G_{ijkl}e_{kl} \quad . \tag{6}$$

For D_{3d} as well as for C_{3v} symmetry, there are only eight independent components for the spin-lattice coupling tensor G.[15] We note that the trace is not an observable and set it equal to zero; thus, the number of independent components is reduced to six.

For large enough axial component to the crystal field, the triplet defined by Eq. (4) is split such that the singlet is isolated from the doublet,[1,13] in which case the frequency of the transition is, to second order,[1]

$$h\nu = 2g_{\parallel}\beta H_z + 8\Delta^2/h\nu_0 \quad , \tag{7}$$

where $h\nu_0$ is the unperturbed Zeeman splitting and Δ is the distribution in the strain amplitudes which mixes only the states of the doublet:

$$\Delta = \tfrac{1}{2}(\tfrac{1}{2}\tau_0 - i\tau_6) \quad , \tag{8}$$

where

$$\tau_0 = \tau_{11} - \tau_{12} \text{ and } \tau_6 = \tau_{12} \quad .$$

In terms of the strain amplitudes, the relevant tensor components are, using the Voigt[16] notation,

$$\tau_0 = (G_{11} - G_{12})(e_1 - e_2) + 2G_{14}e_4 \tag{9a}$$

and

$$\tau_6 = G_{14}e_5 + \tfrac{1}{2}(G_{11} - G_{12})e_6 \ . \tag{9b}$$

The matrix element coupling the states of the doublet for an EPR experiment is shown in Appendix A to be

$$|\langle\rangle|^2 = 16[g_{\parallel}^2\beta^2H_{rf}^2/(h\nu_0)^2]\,\Delta^2 \quad . \tag{10}$$

The factor Δ is that given by Eq. (8) and is thus a distribution function in the strain amplitudes. Consistent with the assumption that the perturbing local strains are random, we specify the probability distribution for each of the six strain components as a Gaussian:

$$p_i(e_i) = (\lambda_i/\pi^{1/2})e^{-\lambda_i^2 e_i^2} \quad . \tag{11}$$

The mathematics can be considerably simplified by noting from Eqs. (9) that τ_0 and τ_6 are independent linear combinations of five of the six independent strain components. From Eqs. (3), (7), and (10), it is seen that the strains occur in the calculation only in the form of Eq. (8). We may therefore transform the integral in Eq. (3) from an integral over a six to an integral over the two-dimensional configuration space defined by τ_0 and τ_6. Equation (3) may now be written in the equivalent form

$$I(E) = \kappa \int_{-\infty}^{\infty} (\tfrac{1}{4}\tau_0^2 + \tau_6^2)\, G[E - (2/h\nu_0)(\tfrac{1}{4}\tau_0^2 + \tau_6^2)] \times \prod_{i=0,6} P_i(\tau_i)\, d\tau_i \quad , \tag{12}$$

where

$$\kappa = 4g_{\parallel}^2\beta^2H_{rf}^2/(h\nu_0)^2 \quad , \tag{13}$$

$$P_0(\tau_0) = \int_{-\infty}^{\infty} \delta[\tau_0 - a_2(e_1 - e_2) - 2a_1e_4] \prod_{i=1}^{6} p_i(e_i)\, de_i \quad ,$$

and

$$P_6(\tau_6) = \int_{-\infty}^{\infty} \delta(\tau_6 - a_1e_5 - \tfrac{1}{2}a_2e_6) \prod_{i=1}^{6} p_i(e_i)\, de_i \quad . \tag{14}$$

Here, we have

$$a_1 = G_{14}, \quad a_2 = G_{11} - G_{12} \quad , \tag{15}$$

and the first factor in the integrand in each expression, Eqs. (13) and (14), is the appropriate projection operator in the form of the Dirac δ function.

The method of performing the indicated integrals in Eqs. (13) and (14) is shown in Appendix B, and the results are

$$P_0(\tau_0) = (\gamma_0/\pi)^{1/2}e^{-\gamma_0\tau_0^2} \tag{16}$$

and

$$P_6(\tau_6) = (\gamma_6/\pi)^{1/2}e^{-\gamma_6\tau_6^2} \quad . \tag{17}$$

The new parameters γ_0 and γ_6 are thus the distribution parameters for the variables τ_0 and τ_6, respectively. These new distribution parameters are given in Appendix B in terms of the local strain distribution parameters and the spin-lattice coupling coefficients.

We consider now two special cases: Case A, where the bulk-crystal symmetry is cubic, and case B, where the bulk-crystal symmetry and the local-site symmetry are the same.

Case A. We calculate the mean square deviation of τ_0 and τ_6 with the strain components referred to the crystal axes. We make the cubic approximation that the diagonal intrinsic strain distributions are all equal and the off-diagonal ones are likewise equivalent. It is easily shown that this leads to the relation

$$\gamma_6 = 4\gamma_0 = \gamma \ . \tag{18}$$

Case B. In this case, we have no real physical basis for establishing an equivalence relation between the distribution parameters γ_0 and γ_6. In order to simplify the integration of the equation for the absorption, Eq. (12), we here impose the equivalence relation calculated for case A. The effect is then a one-parameter instead of a two-parameter model, where the one parameter γ is an averaging of γ_0 and γ_6.

We consider first the case where the lifetime broadening and the width of the inhomogeneous absorption are such that $G(E)$ in Eq. (12) may be taken as the δ function, i.e., $G(E) = \delta(E)$. If we change to polar coordinates, Eq. (12) becomes

$$I(E) = (\kappa/\pi)(\gamma_6\gamma_0)^{1/2} \int_0^{2\pi}\int_0^{\infty} d\theta\, dr\, r^3\delta(E - \alpha r^2) \times \exp(-\gamma_6 r^2\cos^2\theta)\exp(-4\gamma_0 r^2\sin^2\theta) \ , \tag{19}$$

where $\alpha = 2/h\nu_0$. Making the substitution $x = r^2$ and using the relation (18), we have

$$I(E) = 2\kappa\gamma \int_0^{\infty} dx\, x\delta(E - \alpha x)e^{-\gamma x} \ . \tag{20}$$

Thus, we find that

$$I(E) = \frac{2\kappa\gamma}{\alpha}\left(\frac{E}{\alpha}\right)e^{-\gamma E/\alpha} \quad \text{for EPR.} \tag{21}$$

If the spin transitions are induced by phonons (i.e., APR), the matrix element appearing on the right-hand side in Eq. (3) is given by[17]

$$\langle i\,|\,\mathcal{H}_{rf}\,|f\rangle = \langle i\,|\,\vec{S}\cdot\vec{\vec{D}}(t)\cdot\vec{S}\,|f\rangle \quad , \tag{22}$$

to lowest order in the spin operator $\vec{S}$ compatible with the requirement for time-inversion invariance for the Hamiltonian in the absence of an applied mag-

netic field. Here, $\overleftrightarrow{D}(t)$ is the dynamic spin-phonon coupling tensor, the elements of which can be written as a linear combination of the time-varying strain components. Since Eq. (22) is second order in the spin operators, the transition occurs in first order for a non-Kramers doublet and is very nearly independent of the mixing of the states due to the static crystal-field perturbations. Therefore, the matrix element appearing in the integral on the right-hand side in Eq. (3) is a constant of the integration. Thus, Eq. (3) becomes

$$I(E)=\kappa'\int_{-\infty}^{\infty}G[E-(2/h\nu_0)(\tfrac{1}{4}\tau_0^2+\tau_6^2)]\textstyle\prod_i P_i(\tau_i)\,d\tau_i \quad , \tag{23}$$

where κ' is a number appropriate to the particular direction of propagation of ultrasonic waves in the crystal. Transforming to polar coordinates and integrating gives

$$I(E)=2\kappa'(\gamma/\alpha^2)e^{-\gamma E/\alpha} \quad \text{for APR.} \tag{24}$$

Comparing Eqs. (24) and (21), we observe that there is a basic difference between the EPR and APR line shapes, as expected. This is easily seen as a direct consequence of the entirely different mechanisms stimulating the same kind of transition.

Equation (24) does not fit observed spectra very well, at least in some cases.[18] Let us now consider a Gaussian homogeneous distribution $G(\delta E)$ in Eq. (3),

$$G(E-E')=(\sigma/\pi^{1/2})\exp\{-\sigma^2[E-\alpha(\tfrac{1}{4}\tau_0^2+\tau_6^2)]^2\} . \tag{25}$$

Equation (25) may actually be considered the convolution of the distribution resulting from the homogeneous lifetime broadening and any other distribution which causes a symmetric broadening of the resonance line not caused directly by local crystal-field perturbations. There may be, for example, such extraneous interactions which cause unresolved hyperfine or exchange broadening. Equation (25) will be referred to in future discussion simply as the "homogeneous" distribution. Equation (12) is now written as

$$I(E)=(4\kappa\gamma\sigma/\pi^{3/2})e^{-\sigma^2E^2}\int_0^{2\pi}\int_0^{\infty}d\theta\,dr\,r^3e^{-\gamma r^2}\times\exp[-\sigma^2(\alpha^2r^4-2\alpha Er^2)] \quad , \tag{26}$$

where we have again transformed to polar coordinates as was done for Eq. (19). Now let

$$a=\sigma^2\alpha^2, \quad b=2\alpha\sigma^2E, \quad c=\gamma-b. \tag{27}$$

We now have

$$I(E)=(2\kappa\gamma\sigma/\pi^{1/2})e^{-\sigma^2E^2}\int_0^{\infty}dr\,r^3\exp(-ar^4-cr^2) . \tag{28}$$

This may be written in the form

$$I(E)=(2\kappa\gamma\sigma/\pi^{1/2})e^{-\sigma^2E^2}\int_0^{\infty}dx\,x\exp(-ax^2-cx) . \tag{29}$$

The last integral is easily performed, resulting in the expression for the line shape

$$I(E)=\frac{2\kappa\gamma\sigma}{\pi^{1/2}}e^{-\sigma^2E^2}\left\{\frac{1}{2a}-\frac{c}{4a}\left(\frac{\pi}{a}\right)^{1/2}e^{c^2/4a}\left[1-\Phi\left(\frac{c}{2a^{1/2}}\right)\right]\right\} \quad \text{for EPR.} \tag{30}$$

Here, $\Phi(z)$ is the error function. It is to be noted that for an arbitrarily narrow homogeneous distribution, one gets from Eqs. (30) and (27)

$$I(E)\xrightarrow[\sigma\to\infty]{}\frac{2\kappa\gamma}{\alpha}\left(\frac{E}{\alpha}\right)e^{-\gamma E/\alpha}, \quad E>0 \tag{31}$$

as expected.

If we consider now the APR line shape, where the matrix element in Eq. (3) results from (22) and is thus independent of the mixing of the states of the doublet by local crystal-field perturbations, we get the following expression for the line shape:

$$I(E)=(2\kappa'\gamma\sigma/\pi^{1/2})e^{-\sigma^2E^2}\int_0^{\infty}dx\exp(-ax^2-cx) . \tag{32}$$

This integral is easily carried out to give

$$I(E)=2\kappa'\gamma\sigma/\pi^{1/2}e^{-\sigma^2E^2}\left\{\frac{\pi^{1/2}}{2\sigma\alpha}e^{c^2/4a}\left[1-\Phi\left(\frac{c}{2\sqrt{a}}\right)\right]\right\} \tag{33}$$

for APR which is compared with Eq. (24). For an arbitrarily narrow homogeneous distribution we have

$$I(E)\xrightarrow[\sigma\to\infty]{}2\kappa'(\gamma/\alpha^2)e^{-\gamma E/\alpha}. \tag{34}$$

Figure 1 shows the theoretical EPR absorption derivative, and Fig. 2 shows the theoretical APR absorption calculated from Eqs. (30) and (33), respectively. Hypothetical values were taken for the homogeneous-distribution parameter σ and for the strain parameter γ. Comparison of Figs. 1 and 2, which were calculated for the same values of the parameters σ and γ, shows the distinctive comparative features anticipated on the basis of the model between the EPR and APR line shapes. The position of the peak of the undisplaced Zeeman absorption is indicated in Figs. 1 and 2 as the g position. This is the position at which the "g value" for the resonance should be taken on the basis of the model.

B. Site Symmetry C_{3v}: Electric Dipole Transitions

For this case, we still have the Hamiltonian [Eq. (4)] from which we obtain the resonance frequency Eq. (7). We assume that there are no strong applied stationary electric fields present. In this case, the initial wave functions for the states of the doublet have both even- and odd-parity components,

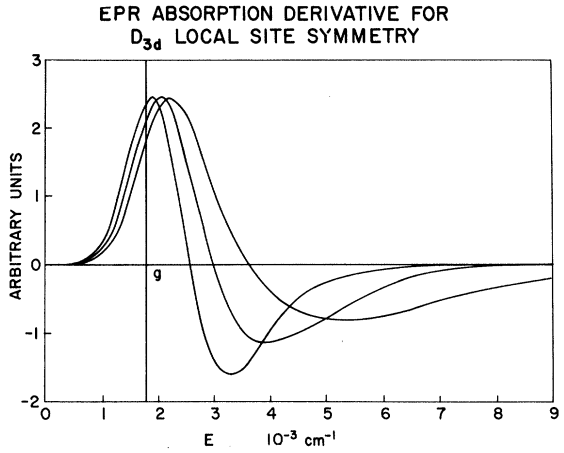

FIG. 1. EPR-absorption derivative for D_{3d} site symmetry for three different values of the intrinsic strain distribution parameter. The homogeneous distribution parameter for the three cases is $\sigma^{-1}=0.667\times10^{-3}\,\mathrm{cm}^{-1}$. The intrinsic strain distribution parameters for the narrow, intermediate, and broad absorption curves are, respectively, $\alpha\gamma^{-1}=0.513\times10^{-3}\,\mathrm{cm}^{-1}$, $9.946\times10^{-3}\,\mathrm{cm}^{-1}$, and $1.67\times10^{-3}\,\mathrm{cm}^{-1}$. The position of the "$g$ value" for the absorption distributions, i.e., the position of the peak of the undisplaced homogeneous distribution, is indicated in the figure by the vertical line.

so that an electric field $\mathcal{E}$ can have a first-order effect.[19] If the transitions are induced in a radiation field, such as would occur in a microwave cavity for instance, the matrix element governing the transition probability is given in Appendix A. In a region of a microwave cavity where the magnetic field component $H_{rf}=0$, we have effectively

$$|\langle i|\mathcal{H}_{rf}|f\rangle|^2=\mathcal{E}_{rf}^2R^2(1-2\Delta^2/\Gamma^2)\ , \tag{35}$$

where R is the spin-electric-field coupling, $\mathcal{E}_{rf}$ is the maximum value of the time-varying electric field, 2Γ is the unperturbed Zeeman term, and Δ is the perturbation distribution given by Eq. (8). The line shape is thus seen to be the proper linear combination of Eqs. (30) and (33). Thus, we have for the piezoparamagnetic resonance (PER) line shape

$$I(E)=\frac{\kappa'\gamma\sigma\alpha^2}{8\pi^{1/2}a}e^{-\sigma^2E^2}\left\{\frac{\pi^{1/2}}{2a^{1/2}}(16\sigma^2+c)\times\left[1-\Phi\left(\frac{c}{2\sqrt{a}}\right)\right]e^{(c^2/4a)}-1\right\} \tag{36}$$

for PER where

$$\kappa'=\mathcal{E}_{rf}^2R^2.$$

The PER line shape from Eq. (36) is shown in Fig. 3, where the values of the parameters λ and σ are the same as those used in Figures 1 and 2.

The position of the peak of the undisplaced Zeeman absorption is indicated in the figure as the g position. This is the position at which the g value for the resonance should be taken on the basis of the model. When Fig. 3 is compared with Figs. 1 and 2, it is seen that the PER linewidth is very nearly the same as that for the APR line in Fig. 2. This is, of course, a direct manifestation of the fact that the mixing of the states by the crystal-field perturbations gives only a second-order contribution in Eq. (35). It is interesting to note that if the sample material is in a region of nonvanishing $\mathcal{E}_{rf}$ and H_{rf}, the line shape is more complicated, i.e., from Appendix A, the transition probability for this case is governed by Eq. (A14). The factor ρ in the next-to-last term in Eq. (A14) is proportional to a linear combination of strains and therefore gives no contribution to the integral (3). The term in the

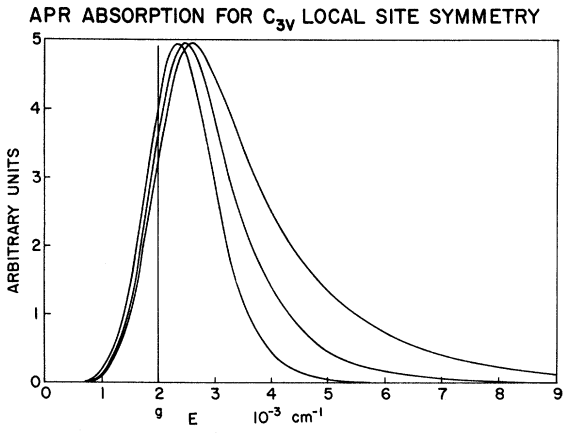

FIG. 2. APR absorption for C_{3v} site symmetry for three different values of the intrinsic strain distribution parameter. The values for the other parameters are those given in Fig. 1.

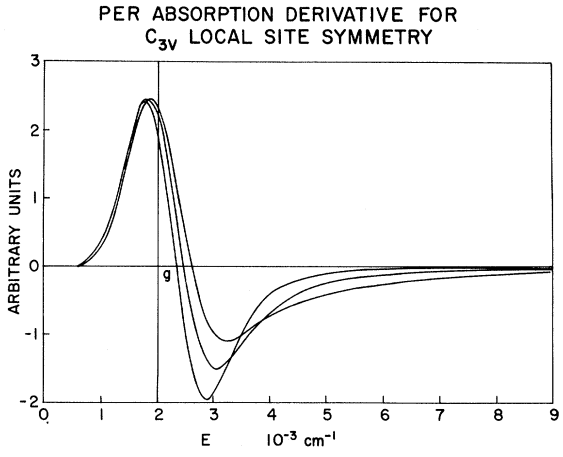

FIG. 3. PER-absorption derivative for C_{3v} site symmetry for three different values of the intrinsic strain distribution parameter. The values for the other parameters are those given in Fig. 1.

difference between σ^2 and ρ^2 gives no net contribution to the line-shape integral; this is discussed in Appendix A. Therefore, we obtain the line shape in this case by adding (30) to (36). The last case discussed is included purely for qualitative purposes, since the requirement of a knowledge of the relative magnetidues of $\mathcal{E}_{rf}$ and H_{rf} makes it comparatively uninteresting from the standpoint of a quantitative evaluation of the parameters of the model from an experimental line shape.

C. O_h Symmetry: Magnetic Quadrupole and Phonon-Induced Transitions

We again consider the lowest-order nontrivial spin manifold for the ground state of a non-Kramers ion compatible with Kramers theorem and time invariance for that part of the Hamiltonian which is independent of any externally applied magnetic field, namely, a triplet.[1] The triplet is not split in the octahedral symmetry; therefore, we must consider explicitly the mixing of the singlet into the states of doublet, even when the degeneracy is raised by an externally applied magnetic field and/or crystal-field perturbations. Thus, there exist two distinct conditions which are expected to give entirely different line shapes for microwave absorption, one with the rf field $\vec{H}_{rf}$ parallel to the applied field $\vec{H}_0$ and the other with $\vec{H}_{rf}$ perpendicular to $\vec{H}_0$. In the first case, the transition probability is nonzero only if the states of the doublet are mixed, say by crystal-field perturbations; in the latter case, the transition probability is dependent entirely on the mixing of the singlet into the states of the doublet.

A calculation similar to this one has been done by McMahon[11] for $\vec{H}_{rf}$ perpendicular to the applied field $\vec{H}_0$. In that calculation, the strain probability distributions were represented as Lorentzian. We present here our calculations for the line shape for both cases, $\vec{H}_{rf}$ parallel and perpendicular. We assume a Gaussian probability distribution for the strains in order to be consistent with the initial assumption that the local crystal-field perturbations can be considered random. Under this assumption, we give also the APR line-shape calculation for comparison.

Consider the spin Hamiltonian for effective spin-1 and octahedral symmetry,

$$\mathcal{H} = g\beta\vec{H}\cdot\vec{S} + \vec{S}\cdot\vec{\vec{D}}\cdot\vec{S} \ , \tag{37}$$

where the second term is added as a perturbation on the first. The last term is used to describe local crystal-field perturbations, and thus the elements of the coupling tensor $\vec{\vec{D}}$ can each be written as a linear combination of the local strain components as in the previous cases. We may consider the perturbing Hamiltonian in the form

$$\mathcal{H}' = \vec{S}\cdot\vec{\vec{D}}\cdot\vec{S} = D_{33}S_3^2 + \Delta S_+^2 + \Delta^* S_-^2 + \Delta'(S_+S_3 + S_3S_+) + \Delta'^*(S_-S_3 + S_3S_-) + \tfrac{1}{4}(D_{11} + D_{22})(S_+S_- + S_-S_+) \ , \tag{38}$$

where

$$\Delta = \tfrac{1}{4}(D_{11} - D_{22} - 2iD_{12}) \tag{39}$$

and

$$\Delta' = \tfrac{1}{2}(D_{13} - iD_{23}). \tag{40}$$

Considering only transitions within the non-Kramers doublet, i.e., $|\Delta M_s| = 2$, the resonance frequency, to second order, is obtained from Eq. (37), and the result is

$$h\nu = 2g\beta H_0 + (8/h\nu_0)(\Delta^2 + \Delta'^2) \ , \tag{41}$$

where $h\nu_0 = 2g\beta H_0$ is the unperturbed Zeeman splitting. Thus, the correction E' to the transition energy is

$$E' = (8/h\nu_0)(\Delta^2 + \Delta'^2) \ . \tag{42}$$

Expanding each element of the tensor $\vec{\vec{D}}$ in terms of the local strain components

$$D_{ij} = \sum_{kl} G_{ijkl} e_{kl} \tag{43}$$

and using Eqs. (39) and (40), Eq. (42) can be written explicitly in terms of the local strain components and the spin-lattice coupling parameters:

$$E' = (8/h\nu_0)\left[\tfrac{9}{8}G_{11}^2(e_{11} - e_{22})^2 + 2G_{44}^2(e_{12}^2 + e_{31}^2 + e_{23}^2)\right], \tag{44}$$

where the number of independent components of the coupling tensor have been reduced to two by setting the trace equal to zero and by requiring that G be invariant under all symmetry operations compatible with the unperturbed local crystal-field symmetry.

Let

$$\alpha' = (h\nu_0)^{-1}, \quad a = \tfrac{9}{8}G_{11}^2, \quad b = \tfrac{1}{2}G_{44}^2 \ . \tag{45}$$

The intrinsic strain broadening for non-Kramers ions in octahedral symmetry where the transition is within a doublet [10] is expected to exhibit considerable broadening. This is seen from the fact that both crystal field mixing of the states of the doublet and mixing of the singlet into the doublet states are of about equal importance. This is contrasted with the condition where the ion site has C_{3v} symmetry with strong axial distortion, treated in Sec. IIA. In the latter case, the influence of the singlet on the resonance frequency for transitions within the doublet is small and may even be neglected. Thus, there should be a tendency toward greater intrinsic broadening for non-Kramers ions in O_h symmetry. Since the intrinsic strain broadening is expected to be dominant, we represent $G(E)$ in Eq. (3) by a δ function, i.e.,

$$G(E) = \delta(E) \ . \tag{46}$$

The resonance absorption for the APR line shape in this case is thus

$$I(E)=\kappa'\tfrac{1}{8}[(\lambda_1\lambda_2/\pi)]^3\int_{-\infty}^{\infty}de_1,\ldots,de_6\,\delta\{E-\alpha[a(e_1-e_2)^2+b(e_4^2+e_5^2+e_6^2)]\}\exp[-\lambda_1^2(e_1^2+e_2^2+e_3^2)]\times\exp[-\tfrac{1}{4}\lambda_2^2(e_4^2+e_5^2+e_6^2)]\,, \quad (47)$$

where we have used the contracted Voigt notation[16] and where we have made the cubic approximation that the distributions of the diagonal strains referred to the crystal axes are all identical, and likewise the distributions of the off-diagonal strains are equal. Here, κ' is a factor which enters because of the APR transition probability which is governed by the matrix element between the states of the time-dependent Hamiltonian of the form of Eq. (22). As in Sec. IIA, κ' is a number appropriate to the particular direction of propagation of ultrasonic waves in the crystal.

If we make the transformation

$$u=e_1-e_2,\quad v=e_1+e_2,\quad r^2=e_4^2+e_5^2+e_6^2\,, \quad (48)$$
$$e_4=r\sin\theta\cos\phi,\quad e_5=r\sin\theta\sin\phi,\quad e_6=r\cos\theta\,,$$

Eq. (47) becomes

$$I(E)=2^{1/2}\,\frac{\kappa'\lambda_1^2\lambda_2^3}{\pi^{5/2}}\int_{-\infty}^{\infty}\int_0^{\infty}du\,dr\,r^2\delta[E-\alpha'(au^2+br^2)]\times\exp\left(-\frac{\lambda_1^2}{2}u^2\right)\exp\left(-\frac{\lambda_2^2}{4}r^2\right)\,. \quad (49)$$

Equation (49) may be written in the form

$$I(E)=2^{1/2}(\kappa'\lambda_1^2\lambda_2^3/\pi^{5/2})\int_0^E F(\tau')G(E-\tau')\,d\tau'\,, \quad (50)$$

where

$$F(\tau')=\int_{-\infty}^{\infty}du\,\delta(\tau'-\alpha' au^2)e^{-\lambda_1^2u^2/2} \quad (51)$$

and

$$G(\tau'')=\int_0^{\infty}dr\,r^2\delta(\tau''-\alpha' br^2)e^{-\lambda_2^2r^2/4} \quad (52)$$

with $\tau''=E-\tau'$. The integrals in Eqs. (51) and (52) are easily carried out to give

$$F(\tau')=\frac{1}{(\alpha' a\tau)^{1/2}}\exp\left(-\frac{\lambda_1^2}{2\alpha' a}\tau'\right) \quad (53)$$

and

$$G(\tau'')=\frac{1}{2(\alpha' b)^{3/2}}\tau''^{1/2}\exp\left(-\frac{\lambda_2^2}{4\alpha' b}\tau''\right)\,. \quad (54)$$

Substitution of Eqs. (53) and (54) into Eq. (50) yields the expression

$$I(E)=\frac{\kappa'\lambda_1^2\lambda_2^3}{2^{1/2}\pi^{5/2}\alpha'^2(ab^3)^{1/2}}\,e^{-\lambda_1^2E/4\alpha' b}\int_0^E d\tau\times\frac{(E-\tau)^{1/2}}{\tau^{1/2}}\exp\left[-\frac{1}{2\alpha'}\left(\frac{\lambda_1^2}{a}-\frac{\lambda_2^2}{2b}\right)\tau\right]. \quad (55)$$

Let

$$p=\frac{\lambda_2^2}{4\alpha' b},\quad q=\frac{\lambda_1^2}{2\alpha' a},\quad c=q-p; \quad (56)$$

the integral in Eq. (55) is performed to give

$$I(E)=\frac{\kappa'\lambda_1^2\lambda_2^3}{2^{1/2}\pi^{5/2}\alpha'^2(ab^3)^{1/2}}\times Ee^{-pE}[B(\tfrac{3}{2},\tfrac{1}{2})\,{}_1F_1(\tfrac{1}{2},2;-cE)]\quad\text{for APR.} \quad (57)$$

Here, B is the beta function,[20] and ${}_1F_1$ is a degenerate hypergeometric series in the argument. The APR absorption given by Eq. (57) is shown in Fig. 4, where, for convenience, we have set equal the two strain distribution parameters λ_1 and λ_2. The absorption curves are shown for three different values of the strain parameter $\bar{\lambda}$.

We turn our attention now to the EPR absorption, and consider first the case where the microwave rf magnetic field $\vec{H}_{rf}$ is oriented perpendicular to the applied dc field $\vec{H}_0$. We have taken the direction of the quantization z along the direction of the applied field H_0. The Hamiltonian for the rf field involves terms in S_+ and S_-. In order to get a nonzero matrix element, we must therefore consider the mixing of the singlet into the states of the doublet. Then, using first-order corrections to the spin functions, we have

$$|\langle i|\mathcal{H}_{rf}|f\rangle|^2=2G_{44}^2H_{rf}^2/(h\nu_0)^2(e_5^2+e_4^2),\quad \vec{H}_{rf}\perp\vec{H}_0. \quad (58)$$

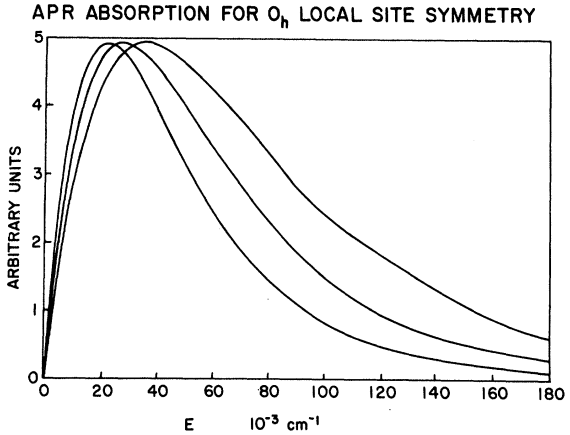

FIG. 4. APR absorption for O_h site symmetry for three different values of the intrinsic strain distribution parameter. The diagonal and off-diagonal intrinsic strain distribution parameters λ_1 and λ_2 were set equal for convenience, giving a one parameter strain distribution $\bar{\lambda}$. The three values for $\bar{\lambda}^{-1}$ for the narrow, intermediate, and broad absorption curves are $\bar{\lambda}^{-1}=1.11\times10^{-4}$, 1.25×10^{-4}, and 1.43×10^{-4}, respectively. The values for the spin-lattice coupling parameters G_{11} and G_{44} were taken as 720 and 460 cm^{-1}/(unit strain), respectively. These values correspond to an average (see Ref. 11) of experimental values reported in the literature.

We proceed in a similar fashion as in the preceding example to obtain the expression for the resonance absorption line shape:

$$I(E)=\frac{\kappa\lambda_1^2\lambda_2^3}{2^{1/2}\pi^{5/2}\alpha'^2(ab^3)^{1/2}}e^{-pE}\int_0^E d\tau\,\frac{(E-\tau)^{3/2}}{\tau^{1/2}}e^{-c\tau}, \tag{59}$$

where

$$\kappa=2G_{44}^2H_{rf}^2/(h\nu_0)^2. \tag{60}$$

Taking the integral in Eq. (60) gives

$$I(E)=\frac{\kappa\lambda_1^2\lambda_2^3}{2^{1/2}\pi^{5/2}\alpha'^2(ab^3)^{1/2}}\times E^2e^{-pE}[B(\tfrac{5}{2},\tfrac{1}{2})_1F_1(\tfrac{1}{2},3;-cE)]$$

for EPR, $\vec{H}_{rf}\perp\vec{H}_0$. (61)

The derivative of Eq. (61) is shown in Fig. 5 for three values of the strain parameter $\bar{\lambda}$. We have again arbitrarily equated the diagonal strain parameter λ_1 with the off-diagonal one λ_2 to yield a single parameterization for the intrinsic strains $\bar{\lambda}$.

We consider now the absorption line shape when the rf magnetic field $\vec{H}_{rf}$ is oriented parallel to the applied dc field $\vec{H}_0$. As in the previous case, we use first-order corrections to the spin functions to get

$$|\langle i|\mathcal{H}_{rf}|f\rangle|^2=\frac{4H_{rf}^2}{(h\nu_0)^2}[a(e_1-e_2)^2+be_6^2]. \tag{62}$$

Using the transformation (48), the expression for the absorption line shape becomes

$$I(E)=\frac{2^{1/2}\kappa''\lambda_1^2\lambda_2^3}{\pi^{5/2}}\times\int_{-\infty}^{\infty}\int_{-\infty}^{\infty}\int_0^{\infty}\int_0^{\pi}\int_0^{2\pi}du\,dv\,dr\,d\theta\,d\varphi\times r^2\sin\theta\,(au^2+br^2\cos^2\theta)\times\delta[E-\alpha'(au^2+br^2)]\times\exp[-\tfrac{1}{2}\lambda_1^2(u^2+v^2)]\exp(-\tfrac{1}{4}\lambda_2^2r^2), \tag{63}$$

where

$$k''=4H_{rf}^2/(h\nu_0)^2. \tag{64}$$

The integral in Eq. (63) is carried out in the same way as in the previous calculation to give

$$I(E)=\frac{2\eta}{\alpha^3(ab^3)^{1/2}}E^2e^{-pE}[B(\tfrac{3}{2},\tfrac{3}{2})\times{}_1F_1(\tfrac{3}{2},3;-cE)+\tfrac{2}{3}B(\tfrac{5}{2},\tfrac{1}{2})_1F_1(\tfrac{1}{2},3;-cE)]$$

for EPR, $\vec{H}_{rf}\|\vec{H}_0$, (65)

where

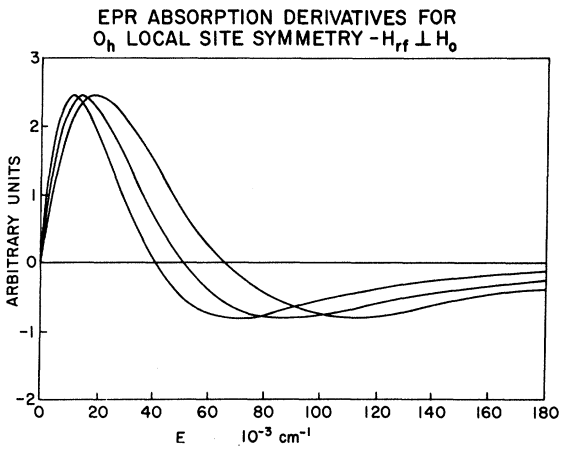

FIG. 5. EPR-absorption derivative for O_h site symmetry and $\vec{H}_{rf}\perp\vec{H}_0$ for three different values of the intrinsic strain distribution parameter $\bar{\lambda}$. The values of the parameters used are those given in Fig. 4.

$$\eta=2^{5/2}\kappa''\lambda_1\lambda_2^3/\pi. \tag{66}$$

The line shape given by Eq. (65) is shown in Fig. 6 as the derivative for the same parameters used for Figs. 4 and 6. Illustrated in Fig. 7 is a normalized comparison of the line shape for $\vec{H}_{rf}\perp\vec{H}_0$ with that for $\vec{H}_{rf}\|\vec{H}_0$. Thus, it is seen that there can be noteworthy discrepancies in the two line shapes depending upon the values for the strain parameters λ_1 and λ_2.

III. DISCUSSION

The results of these calculations are applicable to a variety of materials, the APR and/or the EPR of which have been reported in the literature. For instance, Eqs. (30), (33), and (36) can be applied to $CaF_2:U^{4+}$ where the local axial distortion is caused by local charge compensation or a Jahn-Teller effect.[18,21,22] The superhyperfine structure observed in this material[21] is resolved only at very high magnetic fields, therefore the absorption at low magnetic fields would lend itself quite well to analysis using the Gaussian form for the homogeneous distribution Eq. (25) where the distribution parameter σ is considered the result of the convolution between the lifetime and unresolved superhyperfine broadening.

A second example of the application of Eqs. (33) and (36) is $Al_2O_3:Fe^{2+}$, though only the APR has been reported[6] as yet. The local symmetry of the Al^{3+} ion is actually C_3[23]; however, the deviation from the higher symmetry can be regarded as a slight perturbation. This perturbation amounts to an angle $\theta=4.3°$ which is zero for C_{3v}. Presumably, the Fe^{2+} enters the Al_2O_3 lattice substitutionally.[6]

The APR line shape for $Al_2O_3:Fe^{2+}$ has been analyzed on the basis of Eq. (33), and the agreement

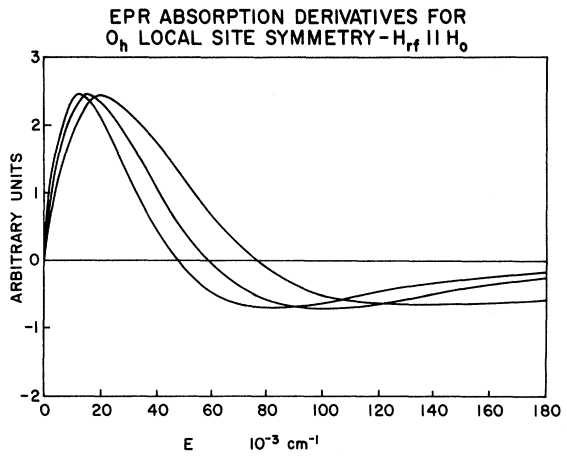

FIG. 6. EPR-absorption derivative for O_h site symmetry and $\vec{H}_{rf} \parallel \vec{H}_0$ for three different values of the intrinsic strain distribution parameter $\bar{\lambda}$. The values of the parameters used are those given in Fig. 4.

is quite good.[24] In this treatment, the PER line shape was predicted using the evaluation of the intrinsic strain parameter from the APR comparison. The effect of uniaxial stress for the PER was also predicted by introducing uniaxial-stress boundary conditions into the model. The comparison with uniaxial-stress measurements offers a means for evaluating the magnitudes of the spin-lattice coupling parameters independently of the concentration of paramagnetic impurity ions.

The results of the calculations for O_h symmetry, Eqs. (57), (61), and (65), are directly applicable to the $|\Delta M_s| = 2$ transition in MgO: Fe^{2+}. We have previously mentioned the work of McMahon[11] in which a line-shape calculation was presented for EPR with $\vec{H}_{rf} \perp \vec{H}_0$. Equation (61) gives a favorable comparison with this previous work, whereas (65) gives the line shape for $\vec{H}_{rf} \parallel \vec{H}_0$ which was not considered in Ref. 11. The intensity of the absorption in the latter case is at least several orders of magnitude stronger than in the former. Also, the $|\Delta M_s| = 1$ and the double quantum line are no longer present with the parallel orientation, and thus the problem of overlap of the absorption lines is eliminated. Equation (57) gives the APR absorption which can be used for the analysis of line-shape comparison studies in conjunction with Eqs. (61) and (65). The results of the calculations were presented taking the intrinsic strain parameters λ_1 and λ_2 equal. The effect of varying the ratio of these parameters is shown in Fig. 8.

IV. CONCLUSION

For conditions where the EPR and APR absorption can be studied on the same sample material, the model presented here provides a means for comparing these line shapes. Conditions of this type have been observed for[21] CaF_2: U^{4+} and[7,8] MgO: Fe^{2+}. Such comparison studies are basic to the understanding of the spin-phonon interaction of paramagnetic impurities in solids,[25] and to the interpretation of the source of the zero-field broadening for non-Kramers doublets.[1]

The assumption, in this model, that the local strains follow random distributions can be justified only by comparing the model with experiment. The qualitative features are certainly in agreement.[6,18] Good quantitative agreement would mean that the sources of strain are, for all practicality, remote.[24]

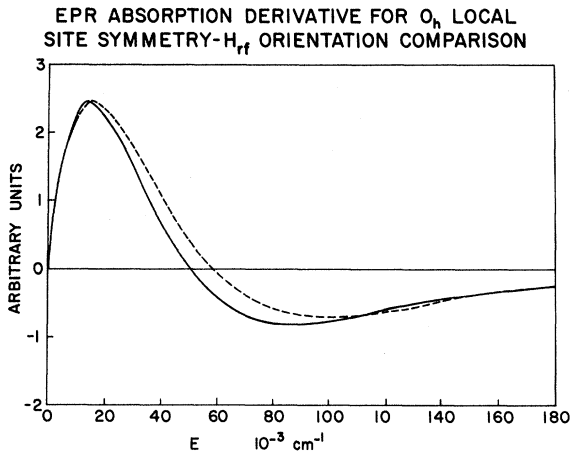

FIG. 7. EPR-normalized absorption derivatives for O_h site symmetry. The solid curve is for $\vec{H}_{rf} \perp \vec{H}_0$ and the dotted one is for $\vec{H}_{rf} \parallel \vec{H}_0$. The value for the strain parameter $\bar{\lambda}^{-1}$ in each case is $\bar{\lambda}^{-1} = 1.25 \times 10^{-4}$ and the other parameters are those used in Fig. 4.

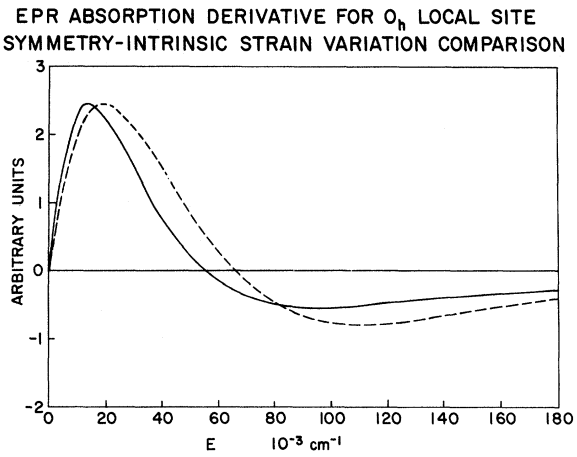

FIG. 8. EPR-absorption derivatives for O_h site symmetry and $\vec{H}_{rf} \parallel \vec{H}_0$. The solid curve corresponds to the values for the intrinsic strain parameters $\lambda_1^{-1} = 1.43 \times 10^{-4}$ and $\lambda_2^{-1} = 1.11 \times 10^{-4}$. The dotted curve has $\lambda_1^{-1} = 1.11 \times 10^{-4}$ and $\lambda_2^{-1} = 1.43 \times 10^{-4}$ for the strain parameters. The spin-lattice parameters are those given in Fig. 4.

The results of the calculations for the line shapes bear out the nature of the matrix element of the Hamiltonian describing the probe which couples the initial and final states. The dissimilarity of the APR as compared to the EPR line shapes as seen in Figs. 1–8 is a direct manifestation of the entirely different mechanisms involved in the two types of experiments. A detailed comparison study, based on the model, can lead to a deeper understanding of these mechanisms.

In cases where the impurity center lacks inversion symmetry, the PER effect may be operative.[19] For C_{3v} symmetry, Eq. (36) provides a means for interpreting the relative strength of the electric field interaction with respect to the spin-phonon coupling.[22]

The model given here for the intrinsic strain-broadened line shapes for non-Kramers doublets has been extended by introducing into the model uniaxial-stress boundary conditions. The results of these calculations will be given in the following paper. In this treatment, the model gives the spin-lattice coupling terms as adjustable parameters, and thus provides a means for evaluating these by comparison with uniaxial-stress experiments, independently of the concentration of the paramagnetic impurity ion. The effect of uniaxial stress for the PER of $CaF_2:U^{4+}$ has been studied experimentally and interpreted on the basis of the model.[26]

ACKNOWLEDGMENT

The authors wish to thank Dr. J. D. Stettler of this laboratory for useful discussions during the course of this work.

APPENDIX A

We wish to calculate the matrix element for the transition probability between the states of the non-Kramers doublet for C_{3v} symmetry. We shall calculate the eigenvalues and eigenfunctions under the assumption that the singlet is far removed from the doublet by the axial component of the crystalline field and ignore any mixing of the singlet into the states of the doublet. Under this assumption, the eigenfunctions for the states of the doublet may be written as

$$\psi_+ = \psi_+^0 + \alpha_3 \psi_-^0 \tag{A1}$$

and

$$\psi_- = \beta_1 \psi_+^0 + \psi_-^0 \ . \tag{A2}$$

The secular determinant of Eq. (4) can then be written in the form

$$\begin{vmatrix} a_{11}-\lambda & 0 & a_{13} \\ 0 & a_{22}-\lambda & 0 \\ a_{31} & 0 & a_{33}-\lambda \end{vmatrix} = 0 \ . \tag{A3}$$

The nontrivial eigenvalues are

$$\lambda_\pm = \mathfrak{D} \pm (\Gamma^2 + 4\Delta^2)^{1/2} \ , \tag{A4}$$

where

$$\mathfrak{D} = \tau_{33} + \tfrac{1}{3} D \ , \tag{A5}$$

$$\Gamma = g_\parallel \beta H_3 \ , \tag{A6}$$

and Δ is given by Eq. (8).

For $\Delta^2/\Gamma^2 \ll 1$, we find that

$$\alpha_3 \approx \Delta/\Gamma \tag{A7}$$

and

$$\beta_1 \approx \Delta^*/\Gamma . \tag{A8}$$

The normalization N is approximately

$$N = (1 + \Delta^2/\Gamma^2)^{-1/2} \ . \tag{A9}$$

If the applied rf magnetic field H_{rf} is taken parallel to the trigonal axis, the Hamiltonian $\mathcal{H}_{rf}$ for the radiation field, including both the magnetic and electric field components, is

$$\begin{aligned} \mathcal{H}_{rf} = {} & g_\parallel \beta H_3(t) S_3 + \tfrac{1}{2} p(t) S_+^2 + \tfrac{1}{2} p^*(t) S_-^2 \\ & + \tfrac{1}{2} q(t) (S_+ S_3 + S_3 S_+) + \tfrac{1}{2} q^*(t) (S_- S_3 + S_3 S_-) \\ & + \tfrac{3}{2} R_{333} \mathcal{E}_3(t) [S_3^2 - S(S+1)] , \end{aligned} \tag{A10}$$

where $p(t) = \alpha + i\beta$ and

$$q(t) = \gamma + i\delta \ . \tag{A11}$$

For C_3 symmetry,[27] we have

$$\begin{aligned} \alpha &= [R_{111} \mathcal{E}_1(t) - R_{222} \mathcal{E}_2(t)] , \\ \beta &= [R_{222} \mathcal{E}_1(t) + R_{111} \mathcal{E}_2(t)] , \\ \gamma &= \tfrac{1}{2} [R_{123} \mathcal{E}_1(t) + R_{113} \mathcal{E}_2(t)] , \\ \delta &= \tfrac{1}{2} [R_{113} \mathcal{E}_1(t) - R_{123} \mathcal{E}_2(t)] . \end{aligned} \tag{A12}$$

In Eqs. (A10) and (A11), $\mathcal{E}_1(t)$ and $\mathcal{E}_2(t)$ are the components of the rf electric field perpendicular to the trigonal axis and $\mathcal{E}_3(t)$ is the axial component. The R_{ijk} are the electric-field-coupling parameters.[27] For C_{3v} symmetry, we may choose the x and y axes such that $R_{111} = 0$; thus,

$$p = -R_{222}(\mathcal{E}_2 - i\mathcal{E}_1) \ . \tag{A13}$$

For convenience, we write $R_{222} = R$ in what follows. If we take $\mathcal{E}_3(t) = 0$, the square of the matrix element for the transition probability between the levels of the doublet is, through second order in Δ/Γ,

$$\begin{aligned} |\langle \rangle|^2 = {} & R^2 \mathcal{E}^2(t) \left[1 - \frac{2}{\Gamma^2} (\Delta^2 - \sigma^2 + \rho^2) \right] \\ & + \frac{4 g_\parallel \beta R H_3(t) \mathcal{E}(t)}{\Gamma} \rho + 4 g_\parallel^2 \beta^2 H_3^2(t) \frac{\Delta^2}{\Gamma^2} , \end{aligned} \tag{A14}$$

where

$$\sigma = \tfrac{1}{4}\tau_0 , \quad \rho = \tfrac{1}{2}\tau_6 \tag{A15}$$

and

$$\mathcal{G}^2(t) = \mathcal{G}_1^2(t) + \mathcal{G}_2^2(t) . \tag{A16}$$

Consider the case where the sample is in a region of high electric field rf intensity so that the magnetic field contribution to (A14) may be neglected. The last two terms are then zero. In the remaining terms, the term in the difference between σ^2 and ρ^2 is easily shown to give no net contribution to the line-shape integral. This can be seen by using Eqs. (A14) and (A15) in Eq. (3), and observing that one gets two integrals, one for σ^2 and the other for ρ^2. Transforming to polar coordinates the integral over the angle θ leaves the same resulting integral in each case but of opposite sign. Thus, the effective form of the matrix element for the line-shape calculation in this case is

$$|\langle\,\rangle|^2_{\text{eff}} = R^2\,\mathcal{G}^2(t)\,[1 - (2/\Gamma^2)\,\Delta^2] . \tag{A17}$$

APPENDIX B

In taking the integrals in Eqs. (13) and (14), we make use of the following theorem.

Given:

$$P_I(\tau_I) = \int_{-\infty}^{\infty} \delta(\tau_I - \sum_{i=1}^{m} c_i e_i) \prod_{i=1}^{m} p_i(e_i)\,de_i , \tag{B1}$$

where the c_i are real numbers and the $p_i(e_i)$ are real functions of the real variables e_i; it follows that

$$P_I(\tau_I) = \frac{1}{\Pi_i |c_i|} \int_{-\infty}^{\infty} dx_1, \ldots, dx_{m-1} p_k\left(\frac{\tau_I - x_1}{c_k}\right) \times p_l\left(\frac{x_1 - x_2}{c_l}\right) \cdots p_q\left(\frac{x_{m-1}}{c_q}\right) , \tag{B2}$$

where $k, l, \ldots, q$ are integers covering the range $i = 1, 2, \ldots, m$ without regard to any particular ordering.

Proof:

Equation (B1) can be rewritten in the equivalent form

$$P_I(\tau_I) = \int_{-\infty}^{\infty} dx_1\, \delta(\tau_I - x_1 - c_k e_k) \times \delta\Big(x_1 - \sum_{\substack{i=1 \\ i\neq k}}^{m} c_i e_i\Big) \prod_{i=1}^{m} p_i(e_i)\,de_i . \tag{B3}$$

We take the integral over e_k to give

$$P_I(\tau_I) = \frac{1}{|c_k|} \int_{-\infty}^{\infty} dx_1 p_k\left(\frac{\tau_I - x_1}{c_k}\right) \times \delta\Big(x_1 - \sum_{\substack{i=1 \\ i\neq k}}^{m} c_i e_i\Big) \prod_{\substack{i=1 \\ i\neq k}}^{m} p_i(e_i)\,de_i . \tag{B4}$$

Similarly, we may rewrite Eq. (B4) in the form

$$P_I(\tau_I) = \frac{1}{|c_k|} \int_{-\infty}^{\infty} dx_1 dx_2 p_k\left(\frac{\tau_I - x_1}{c_k}\right) \times \delta(x_1 - x_2 - c_l e_l)\, \delta\Big(x_2 - \sum_{\substack{i=1 \\ i\neq k,\,l}}^{m} c_i e_i\Big) \times \prod_{\substack{i=1 \\ i\neq k}}^{m} p_i(e_i)\,de_i . \tag{B5}$$

On performing the integration over e_l, Eq. (B5) becomes

$$P_I(\tau_I) = \frac{1}{|c_k|\,|c_l|} \int_{-\infty}^{\infty} dx_1 dx_2 p_k\left(\frac{\tau_I - x_1}{c_k}\right) \times p_l\left(\frac{x_1 - x_2}{c_l}\right) \delta\Big(x_2 - \sum_{\substack{i=1 \\ i\neq k,\,l}}^{m} c_i e_i\Big) \times \prod_{\substack{i=1 \\ i\neq k,\,l}}^{m} p_i(e_i)\,de_i . \tag{B6}$$

We iterate this procedure through $m - 1$ times. Thus, from Eq. (B1) we get Eq. (B2).

Furthermore, we have the following corollary: From Eq. (B2), Eq. (B1) may be written in the form

$$P_I(\tau_I) = \Big[\prod_{i=1}^{m} |\,c_i\,|\Big]^{-1} \int_{-\infty}^{\infty} d\tau'\, G(\tau_I - \tau') F(\tau') , \tag{B7}$$

where

$$G(\tau_I - \tau') = p_k\left(\frac{\tau_I - \tau'}{c_k}\right) \tag{B8}$$

and

$$F(\tau') = \int_{-\infty}^{\infty} dx_2 \ldots dx_{m-1} p_l\left(\frac{\tau' - x_2}{c_l}\right) \times p_p\left(\frac{x_2 - x_3}{c_p}\right) \cdots p_q\left(\frac{x_{m-1}}{c_q}\right) \tag{B9}$$

with the $p_i(e_i)$ given by Eq. (11).

We consider Eq. (13), and using Eq. (B2) or (B7) together with Eqs. (B8) and (B9), we get Eq. (16) as the result after taking the indicated integrals with

$$\gamma_0 = \frac{(\lambda_1 \lambda_2 \lambda_4)^2}{4a_1^2 \lambda_1^2 \lambda_2^2 + a_2^2(\lambda_1^2 + \lambda_2^2)} . \tag{B10}$$

In similar fashion, we get Eq. (17) with

$$\gamma_6 = \frac{(2\lambda_5 \lambda_6)^2}{a_2^2 \lambda_5^2 + 4a_1^2 \lambda_6^2} . \tag{B11}$$

[1]C. M. Bowden, H. C. Meyer, and P. L. Donoho, Inter. J. Quantum Chem. Suppl. 3s, 617 (1970).

[2]B. Bleaney and H. E. D. Scovil, Phil. Mag. 43, 999 (1952); B. Bleaney, P. M. Llewellyn, M. H. L. Price,

and G. R. Hall, Phil. Mag. 45, 991 (1954); U. Ranon and K. Lee, Phys. Rev. 188, 539 (1969).
[3]H. C. Meyer, P. F. McDonald, J. D. Stettler, and P. L. Donoho, Phys. Letters 24A, 569 (1967).
[4]F. I. B. Williams, Proc. Phys. Soc. (London) 91, 111 (1967).
[5]J. W. Culvahouse, D. P. Schinke, and D. S. Foster, Phys. Rev. Letters 18, 117 (1967).
[6]J. Lewiner, P. H. E. Meijer, and J. K. Wigmore, Phys. Rev. 185, 549 (1969).
[7]I. S. Ciccarello, R. Arzt, and K. Dransfeld 138A, 934 (1965).
[8]W. Low, Phys. Rev. 101, 1827 (1956).
[9]S. D. McLaughlan, Phys. Rev. 150, 118 (1966).
[10]The term doublet is used here to denote the $|\Delta M_s| = 2$ transition within a ground triplet.
[11]D. H. McMahon, Phys. Rev. 134, A128 (1964).
[12]A. M. Stoneham, Rev. Mod. Phys. 41, 82 (1969).
[13]C. M. Bowden and H. C. Meyer, Phys. Status Solidi 32, K131 (1969).
[14]K. A. Mueller, Phys. Rev. 171, 350 (1968).
[15]F. G. Fumi, Acta Cryst. 5, 44 (1952).
[16]W. Voigt, *Lehrbuch der Kristallphysik* (Teubner, Leipzig, 1910).
[17]W. J. Dobrov, Phys. Rev. 146, 268 (1966).
[18]P. F. McDonald, Phys. Rev. 177, 447 (1969).
[19]N. Bloembergen, Science 133, 1363 (1961).
[20]J. S. Gradshteyn and J. M. Ryzhik, *Table of Integrals, Series and Products* (Academic Press, New York, 1965).
[21]C. M. Bowden, H. C. Meyer, P. F. McDonald, and J. D. Stettler, J. Phys. Chem. Solids 30, 1535 (1969).
[22]P. K. Wunsch, P. L. Donoho, H. C. Meyer, and C. M. Bowden, Bull. Am. Phys. Soc. 15, 250 (1970).
[23]S. Geschwind and J. P. Remeika, Phys. Rev. 122, 757 (1961).
[24]C. M. Bowden, H. C. Meyer, and P. L. Donoho, Inter. J. Quantum Chem. Suppl. (to be published).
[25]R. Loudon, Phys. Rev. 119, 919 (1960).
[26]P. L. Donoho, P. K. Wunsch, P. F. McDonald, C. M. Bowden, and H. C. Meyer, Bull. Am. Phys. Soc. 15, 250 (1970).
[27]E. B. Royce and N. Bloembergen, Phys. Rev. 131, 1912 (1963).

PHYSICAL REVIEW B VOLUME 3, NUMBER 3 1 FEBRUARY 1971

Effects of Uniaxial Stress on the Magnetic-Resonance Absorption Line Shapes for Non-Kramers Doublets

C. M. Bowden and H. C. Meyer
Solid State Physics Branch, Physical Sciences Laboratory, Redstone Arsenal, Alabama 35809
and
P. L. Donoho
Rice University, Houston, Texas 77001
(Received 18 June 1970)

A model is presented for uniaxial-stress-induced alterations in the intrinsically strain-broadened line shapes for magnetic-resonance absorption within a non-Kramers doublet for the point-group symmetries D_{3d}, C_{3v}, and O_h. (The term *doublet* is used here to denote the $|\Delta M_s| = 2$ transition within a ground triplet.) The uniaxial stress is introduced as boundary conditions in the model for the intrinsically strain-broadened line shapes for non-Kramers doublets given previously. The effects of uniaxial stress are considered for the EPR where the local site symmetry is O_h and D_{3d}. For the local symmetry C_{3v}, the effects of uniaxial stress are considered for the paraelectric resonance absorption. The model provides a means for evaluating the strength of the spin-lattice coupling from uniaxial-stress experiments, independent of the concentration of the paramagnetic impurity ions.

I. INTRODUCTION

Since the initial work done by Watkins and Feher,[1] much interest has been devoted to the determination of the parameters for the spin-lattice interaction for paramagnetic impurities in diamagnetic host lattices by introducing local crystal field perturbations using uniaxial stress. Feher's analysis[2] accounts reasonably well for first-order spectral shifts in the magnetic-resonance absorption for the Kramers ions Mn^{2+} and Fe^{3+} in MgO.

When the lowest-order nonzero contribution of local crystal field perturbations is second order, as it is for transitions within a non-Kramers doublet,[3] the spectral effect of uniaxial stress is quite different. Since the crystal field gives no first-order contributions to transitions within the doublet, the effect on the shape of the resonance line must be explicitly considered. In this paper we give a model for the effect of uniaxial stress on the shapes of intrinsically strain-broadened magnetic-resonance line shapes for transitions within a non-Kramers doublet.[3a] The model is given for the EPR for the local site symmetries O_h and D_{3d}. The case of C_{3v}